



## CASE REPORT

# 3D-printed Bioresorbable Scaffold for Periodontal Repair

G. Rasperini<sup>1</sup>, S.P. Pilipchuk<sup>2,3</sup>, C.L. Flanagan<sup>3</sup>, C.H. Park<sup>4</sup>, G. Pagni<sup>1</sup>, S.J. Hollister<sup>3,5,6</sup>, and W.V. Giannobile<sup>2,3\*</sup>

**Key Words:** dental materials, tissue engineering, bioprinting, periodontal regeneration, selective laser sintering, periodontal ligament.

Tissue-engineered constructs have potential to induce bone-ligament complex regeneration to treat disease- or trauma-induced damage to periodontia (Ivanovski et al. 2014). Herein, we provide the first reported human case of treatment of a large periodontal osseous defect with a 3D-printed bioresorbable patient-specific polymer scaffold and signaling growth factor. The treated site remained intact for 12 mo following therapy. This report suggests that 3D-printed image-based scaffolds offer potential for periodontal reconstruction. Limitations gleaned from this case and opportunities for treatment of other bony defects are discussed.

## Methods and Materials

### Case Presentation

A healthy 53-y-old white man who was diagnosed with generalized aggressive periodontitis presented for treatment to preserve his dentition. The patient received full-mouth scaling/root planing and 2 y later still showed signs of periodontal stability but with a resulting large labial

soft and osseous defect associated with the mandibular left cuspid (Fig. 1, top panels). Given the limited reconstructive options, the patient consented to treatment by a bioengineering approach. The case study was approved by the University of Milan Institutional Review Board.

### 3D-printed Scaffold Fabrication

An STL format was used as an input data file for the manufacturing process and to determine a best fit based on a computed tomography scan of the patient's defect (slice thickness, 400  $\mu\text{m}$ ; voxel size, 400  $\times$  400  $\mu\text{m}$ ). Magics 15 (Materialise Inc., Leuven, Belgium) was used to subtract the STL-generated defect from the designed scaffold to generate a 3D design, which was then further modified using NX 7.5 (Siemens PLM Software, Plano, TX, USA) and Mimics (Materialise Inc; Fig. 1, middle panels). The design consisted of perforations for fixation, an internal port for delivery of recombinant human platelet-derived growth factor BB (rhPDGF-BB), and pegs oriented perpendicularly to the root for periodontal ligament (PDL) formation as previously described using polycaprolactone (PCL) scaffolds in a rodent periodontal defect model (Park et al., 2012; Fig. 1, bottom). Selective laser sintering allows for fabrication

of precise scaffold features that can be designed to support structural and functional tissue regeneration. Selective laser sintering (Formiga P100 System; EOS e-Manufacturing Solutions) was used to 3D-print the scaffold with PCL powder (Polysciences Inc., Warrington, PA, USA; milled at Jet Pulverizer, Moorestown, NJ, USA) containing 4% hydroxyapatite. PCL is a hydrolytically degradable polymer approved by the Food and Drug Administration. Geometric interface adaption of the scaffold to the defect was assessed using a patient-specific 3D-printed prototype model (University of Michigan Medical Innovation Center). Micro-computed tomography scans (eXplore Locus SP, GE Healthcare, London, Canada) of a prototyped mandible with scaffold were used to determine the adaptation ratio based on the methodology for PDL fiber guidance. Measurements of gap distance between the scaffold PDL region and modeled tooth root were repeated ( $n = 3$ ) to determine mean adaptation for in vivo placement (Fig. 1, lower-middle panels; Appendix Fig. 1). The scaffold was sterilized using ethylene oxide (Nelson Laboratories, Salt Lake City, UT, USA). The University of Michigan Institutional Review Board granted exemption status for evaluation of the scaffold matrix.

DOI: 10.1177/0022034515588303. <sup>1</sup>Department of Biomedical, Surgical, and Dental Sciences, Unit of Periodontology, Foundation IRCCS Ca' Granda Polyclinic, University of Milan, Milan, Italy; <sup>2</sup>Department of Periodontics and Oral Medicine, School of Dentistry, University of Michigan, Ann Arbor, MI, USA; <sup>3</sup>Department of Biomedical Engineering, College of Engineering, University of Michigan, Ann Arbor, MI, USA; <sup>4</sup>Department of Nanobiomedical Science & BK21 PLUS NBM Global Research Center for Regenerative Medicine, Dankook University, Cheonan, South Korea; <sup>5</sup>Department of Surgery, School of Medicine, University of Michigan, Ann Arbor, MI, USA; and <sup>6</sup>Department of Mechanical Engineering, College of Engineering, University of Michigan, Ann Arbor, MI, USA; \*corresponding author, wgiannob@umich.edu

A supplemental appendix to this article is published electronically only at <http://jdr.sagepub.com/supplemental>.

**Figure 1.**

A customized scaffold was 3D printed using medical-grade polycaprolactone to fit the periosteous defect using a prototyped model of the defect from the patient's cone beam computed tomography scan. The scaffold's internal region consisted of extended pegs for the support and guidance of periodontal ligament formation, perforations for fixation, and an internal compartment for delivery of recombinant human platelet-derived growth factor BB, as shown in the cross-sectional view. Micro-computed tomography scans of the polycaprolactone scaffold fitted into the prototyped defect model (see coronal, middle, apical views) were used to determine the topographic adaptation of the scaffold to the root surface. PDL, periodontal ligament.

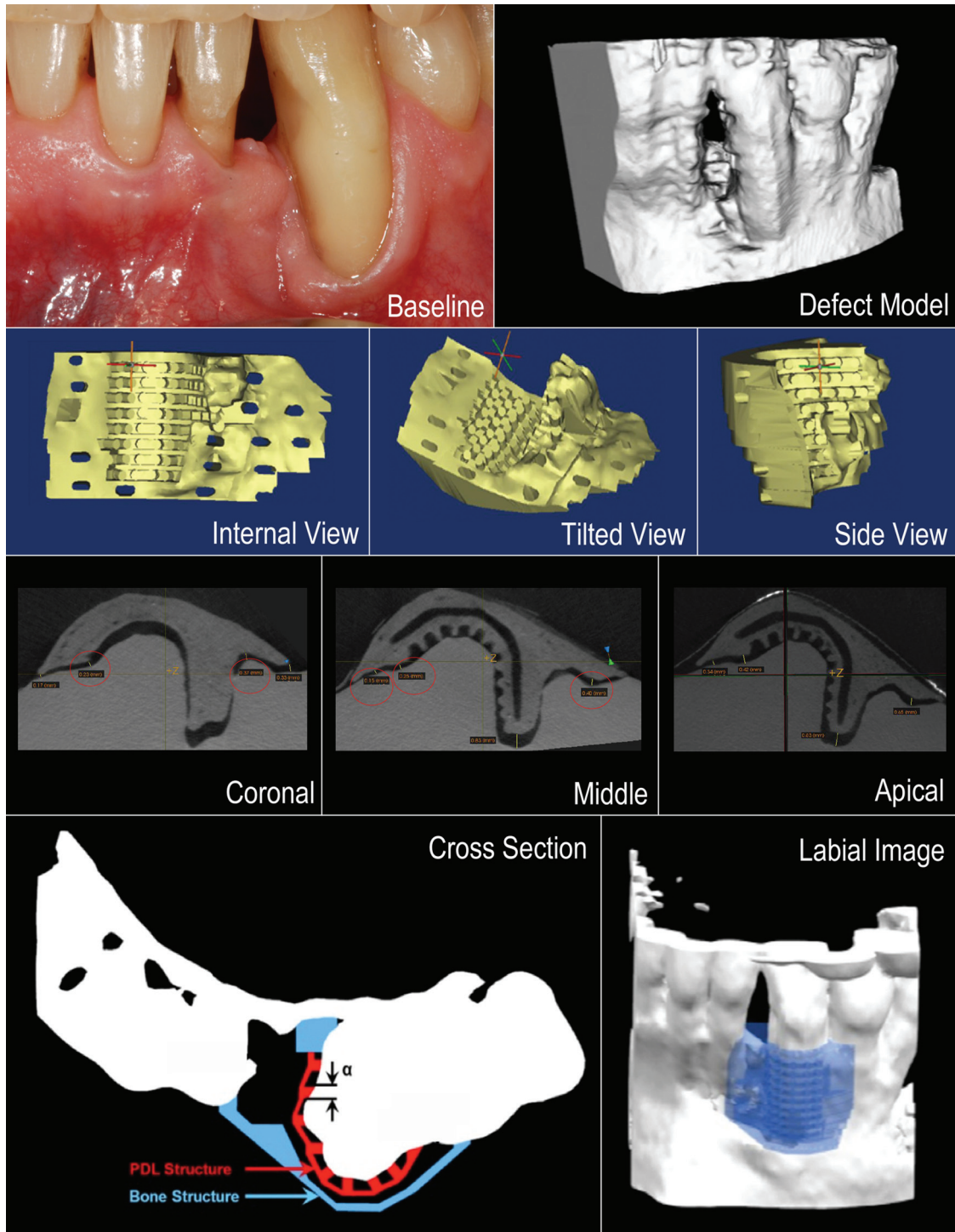
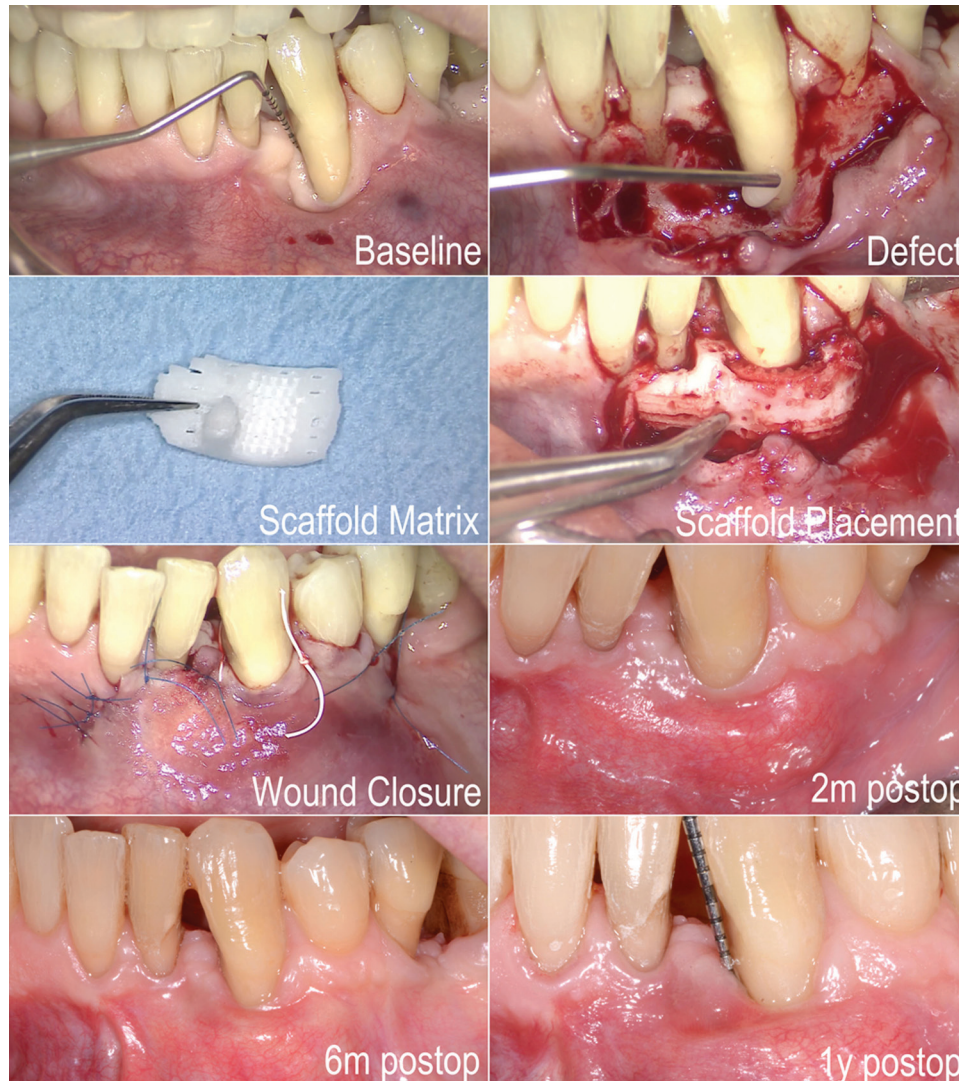


**Figure 2.**

Clinical attachment loss and alveolar ridge resorption characterized the patient's periosteal defect involving tooth No. 22. During root preparation, a trapezoidal full-thickness flap was elevated to expose the defect; the root surface was mechanically instrumented; and the EDTA solution was applied. Prior to implantation, the scaffold matrix was immersed in a solution of recombinant human platelet-derived growth factor BB (0.3 mg/mL) for 15 min at room temperature. During placement, the scaffold was filled with autologous blood, positioned over the exposed tooth root, and stabilized using poly-D and L-lactic acid pins. Tension-free primary intention method was employed during wound closure. The implanted 3D scaffold filled the periodontal osseous defect without clinical signs of chronic inflammation or rejection of the polycaprolactone-based material during the first year.



### Surgical Procedure and Scaffold Delivery

The patient was prepared with local infiltration anesthesia (Fig. 2; video, available online). A trapezoidal full-thickness labial flap was elevated encompassing the adjacent teeth. Vertical incisions were extended beyond the mucogingival junction to allow relaxation of the flap and ease scaffold placement. The tooth root surface was

mechanically instrumented, and EDTA (Straumann PrefGel, Institut Straumann AG, Basel, Switzerland) was used as a root modification agent. The scaffold was immersed in 0.5 mL of rhPDGF-BB (0.3 mg/mL; Gem 21S, Osteohealth, Shirley, NY, USA) for 15 min, filled with autologous blood from the defect site, and stabilized over the defect with ultrasound-activated resorbable poly-D and L-lactic acid pins (SonicWeld, KLS

Martin Group, Tuttlingen, Germany). The rhPDGF-BB solution was also applied directly to the tooth root. The flap was released to allow tension-free primary closure with nonresorbable sutures. The patient refrained from mechanical oral hygiene procedures using 0.12% chlorhexidine rinses for 3 wk. The patient was prescribed amoxicillin (875 mg) and clavulanic acid (125 mg, twice a day for 6 d) and ibuprofen (600 mg) as needed

for pain postoperatively. Sutures were removed 7d following surgery (video).

## Results

The scaffold design incorporated pegs 160 to 380  $\mu\text{m}$  in length consistent with human PDL, with the superior PDL region being shorter to accommodate to root proximity. Mean strut length was 600  $\mu\text{m}$  for support of extensions in the PDL region, while channel width for PDGF delivery was  $\sim 500$   $\mu\text{m}$  (Fig. 1). The interface was determined to have an adaptation ratio of  $0.82 \pm 0.07$ , which characterizes gap width distribution between the scaffold and tissue (Appendix Fig. 1). In vitro release kinetics demonstrated an overall burst delivery of rhPDGF-BB from the matrix over a 3-h period (Appendix Fig. 2).

The scaffold remained covered for 12 mo, demonstrating a 3-mm gain of clinical attachment and partial root coverage (Appendix Table 1). The implanted 3D scaffold served to fill the human periodontal osseous defect without signs of chronic inflammation or dehiscence (Fig. 2). However, at 13 mo, the scaffold became exposed (Appendix Fig. 3). Professional oral hygiene was performed and 0.12% chlorhexidine intrapocket irrigation delivered. A few fragments of the scaffold were removed from the pocket. Amelogenin gel was delivered to the site and subsequently sealed using surgical cyanoacrylate gel. Systemic antibiotics were prescribed (amoxicillin, 875 mg; clavulanic acid, 125 mg; twice a day for 6 d). Twenty days later, the patient presented with a graft exposure 3 mm below the gingival margin. The exposed part of the graft was removed. At 2 wk, the site showed a larger dehiscence and wound failure, necessitating entire scaffold removal (Appendix Fig. 3, middle panels). The scaffold matrix was retrieved, fixed in formalin, and evaluated histologically and for molecular weight assessment. Based on gel permeation chromatography, 75.9% of the scaffold molecular weight remained after 14 mo (Appendix Table 2) with primarily connective tissue healing and minimal evidence of bone repair, as

determined clinically and histologically (Appendix Fig. 3, bottom panels).

## Discussion

When tissue engineering approaches are applied to the reconstruction of complex tissue structures such as the periodontium, biomaterials serve as 3D templates and synthetic extracellular matrix environments for the regenerative process (Tevlin et al. 2014). Printed biomaterials represent promising tools, allowing customization to the desired size, configuration, and architecture of a given defect. Their efficacy in the regeneration of complex structures such as new PDL has been shown preclinically (Park, Rios, et al. 2014). Successful use of a 3D-printed PCL splint for the treatment of tracheobronchomalacia was reported using a similar approach (Zopf et al. 2013). We believe that a limitation of this study was use of the PCL biomaterial that may not be ideal for periodontal applications. It appears that a more rapidly resorbing matrix with a healing window of  $<1$  y combined with a less bulky design would be better suited to avoid wound dehiscence, exposure, and subsequent microbial contamination in a perimucosal environment around teeth. The limited bone regeneration noted histologically suggests the need for a more interconnected, open, internal structure with greater surface area. Selection of a biomaterial with a faster rate of resorption (e.g., polylactic-co-glycolic acid or gelatin; Park, Kim, et al. 2014) combined with a highly porous structure might contribute to improved tissue ingrowth and vascularization. The slow scaffold resorption profile suggests that improvements in the degradation properties could better promote bony infill, which is difficult to achieve with a slowly degrading matrix. Compartmentalized delivery of biologics to the PDL-forming region of the scaffold along with osteogenic molecules (e.g., bone morphogenetic proteins) to the bone region may further facilitate tissue growth and remodeling. Although platelet-derived growth factor BB has been shown to bind and release from a

PCL-based scaffold in a biological manner (Phipps et al. 2012), optimization of the growth factor release kinetics may further increase GF bioactivity in situ.

This case represents the first application of a personalized 3D-printed bioresorbable scaffold to treat a periodontal defect. Although this case was unsuccessful in the long term, we believe that the approach warrants further study for more personalized oral regenerative medicine clinical applications.

## Author Contributions

G. Rasperini, W.V. Giannobile, contributed to conception, design, and data analysis, drafted the manuscript; S.P. Pilipchuk, contributed to data analysis, drafted the manuscript; C.L. Flanagan, contributed to data analysis, critically revised the manuscript; C.H. Park, contributed to conception and design, critically revised the manuscript; G. Pagni, contributed to data analysis, drafted and critically revised the manuscript; S.J. Hollister, contributed to conception, design, and data analysis, critically revised the manuscript. All authors gave final approval and agree to be accountable for all aspects of the work.

## Acknowledgments

This study was supported by the University of Michigan School of Dentistry, Najjar Endowment. S.P.P. is supported by a National Science Foundation Fellowship (DGE 1256260). We thank Jim Sugai for technical assistance. We also thank Quintessence Video Services for its assistance with the video capture. S.J.H., C.H.P., S.P.P., and W.V.G. hold intellectual property relevant to the use of bioprinted scaffolds for oral applications. The authors declare no other potential conflicts of interest with respect to the authorship and/or publication of this article.

## References

- Ivanovski S, Vaquette C, Gronthos S, Huttmacher DW, Bartold PM. 2014. Multiphasic scaffolds for periodontal tissue engineering. *J Dent Res*. 93(12):1212–1221.

Park CH, Kim KH, Rios HF, Lee YM, Giannobile WV, Seol YJ. 2014. Spatiotemporally controlled microchannels of periodontal mimic scaffolds. *J Dent Res*. 93(12):1304–1312.

Park CH, Rios HF, Jin Q, Sugai JV, Padi-al-Molina M, Taut AD, Flanagan CL, Hollister SJ, Giannobile WV. 2012. Tissue engineering bone-ligament complexes using fiber-guiding scaffolds. *Biomaterials*. 33(1):137–145.

Park CH, Rios HF, Taut AD, Padi-al-Molina M, Flanagan CL, Pilipchuk SP, Hollister SJ, Giannobile WV. 2014. Image-based, fiber guiding scaffolds: a platform for regenerating tissue interfaces. *Tissue Eng Part C Methods*. 20(7): 533–542.

Phipps MC, Xu Y, Bellis SL. 2012. Delivery of platelet-derived growth factor as a chemotactic factor for stem cells by bone-mimetic electrospun scaffolds. *PLoS One*. 7(7):e40831.

Tevlin R, McArdle A, Atashroo D, Walmsley GG, Senarath-Yapa K, Zielins ER, Paik KJ, Longaker MT, Wan DC. 2014. Biomaterials for craniofacial bone engineering. *J Dent Res* 93(12):1187–1195.

Zopf DA, Hollister SJ, Nelson ME, Ohye RG, Green GE. 2013. Bioresorbable airway splint created with a three-dimensional printer. *N Engl J Med*. 368(21):2043–2045.